Supplemental Figures

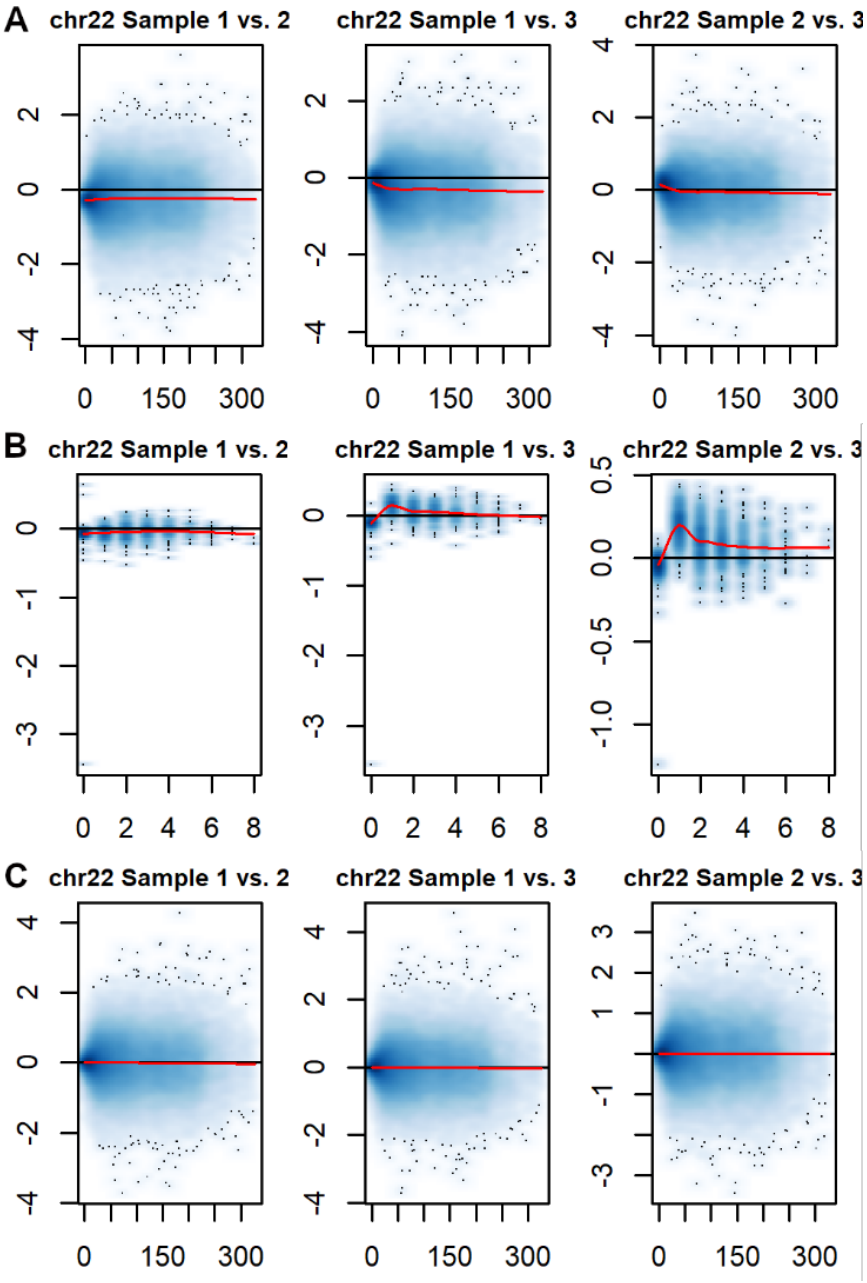

Supplemental Figure S1. MD plots for untreated HCT-116 replicates at 100KB resolution. A) Raw data, B) HiCNorm normalized data, and C) mutliHiCcompare fastlo normalized data. Red lines indicate loess fit to the data. HiCNorm is does not removed between dataset bias while the multiHiCcompare fastlo procedure can remove the between dataset bias. HiCNorm was designed to remove bias due to GC content, fragment size, and mappability however these factors are all very similar or the same between datasets (assuming the data is from the same genome) and do not pose much of an issue when the purpose of normalization is comparison. HiCNorm does not

seem to be able to remove the between dataset technical biases that need to be removed for the purpose of comparison.

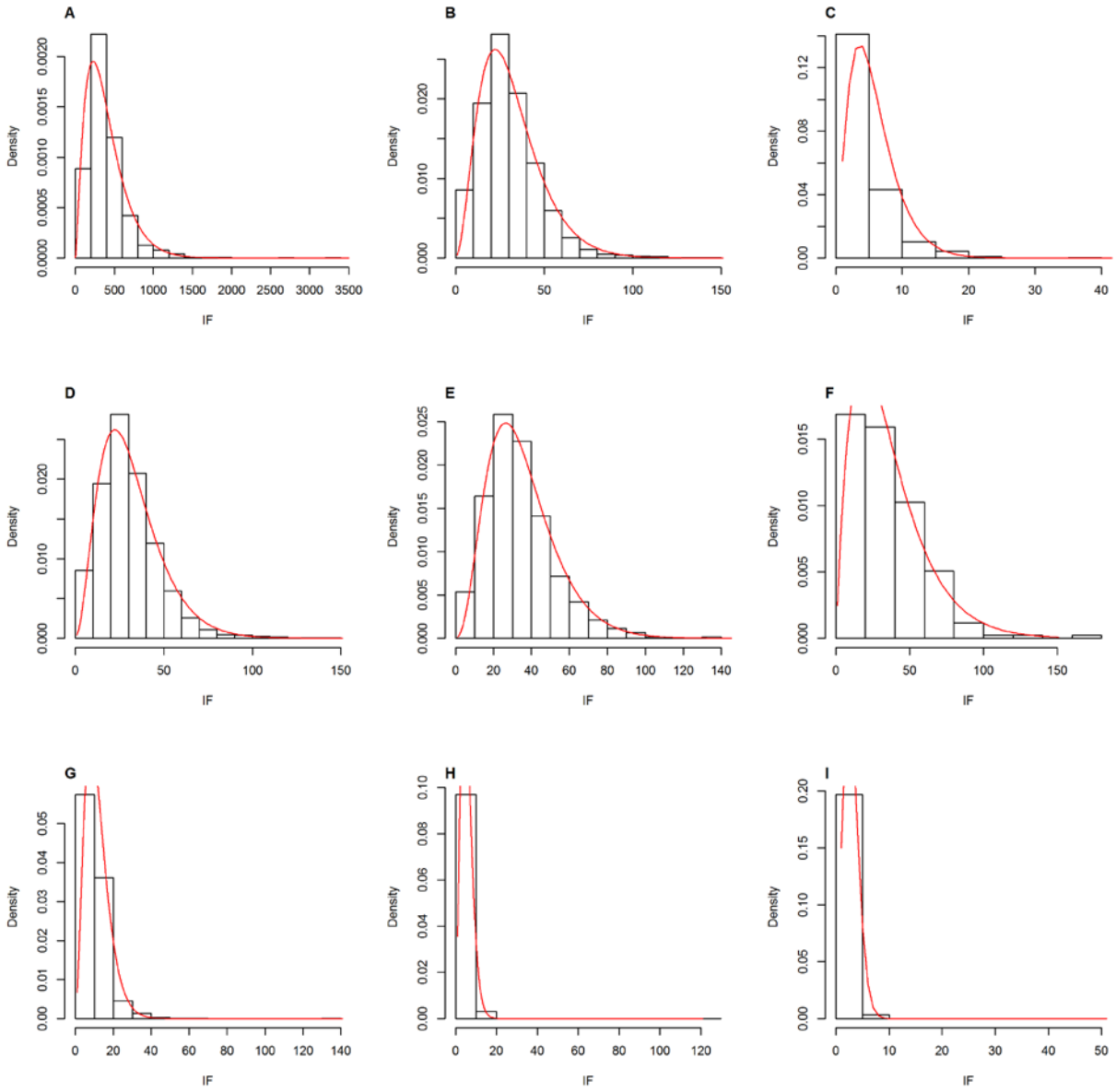

Supplemental Figure S2. Suitability of negative binomial distribution to fit distance-centric chromatin interaction frequencies at different distances, A) Distance = 10, B) Distance = 100, C) Distance = 1000; chromosomes, D) chr1, E) chr18, F) chr19, and resolutions G) 100KB, H) 50KB, I) 10KB. Red lines indicate the theoretical negative binomial distribution using the estimated parameters from the Hi-C data. Histogram bars represent real distribution of the IFs from the Hi-C data. Data for parts A) - F) are from GM12878 cell line (Suhas S P Rao et al. 2014) at 100KB resolution. Data for parts G) - I) are from HCT-116 cell line, chr1.

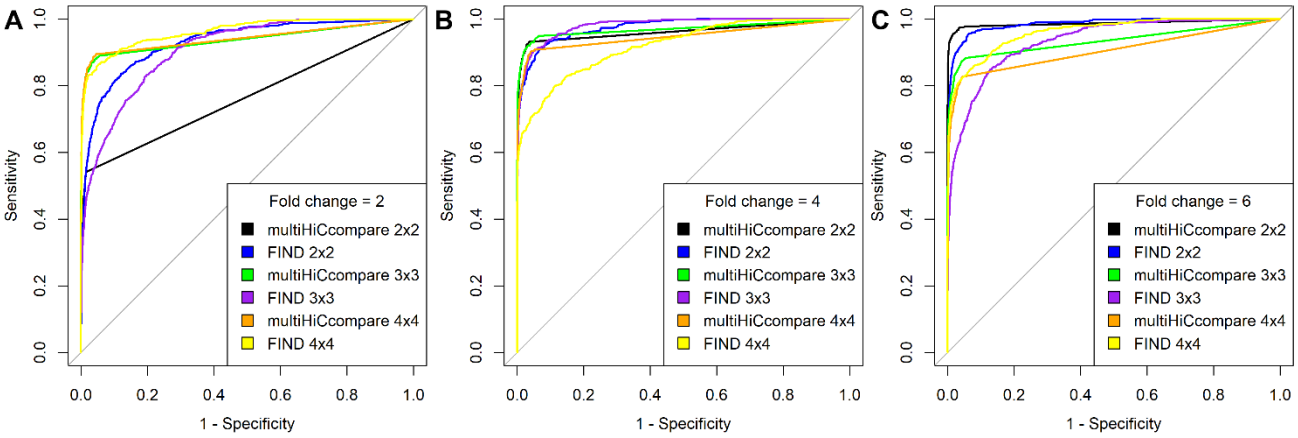

Supplemental Figure S3. ROC analysis for the comparison between multiHiCcompare and FIND over different fold changes and the number of replicates per group. Data were simulated using FIND's simulation function for two conditions with varying numbers of replicates in each condition. Data were then inputted into a FIND and multiHiCcompare analysis and the results were compared with the true differences. A) Fold change = 2, B) fold change = 4, C) fold change = 6.

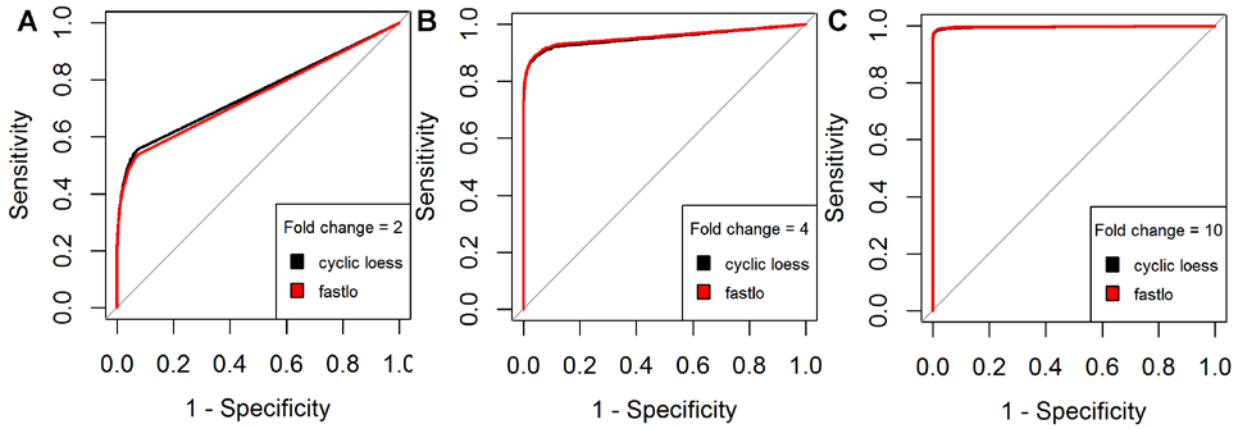

Supplemental Figure S4. ROC analysis for the comparison between cyclic loess and fastlo method. A)-C) ROC curves for the effect of each normalization method on difference detection at fold changes of A) 2, B) 4, C) 10. Analysis performed on data from HCT-116 cell line chromosome 1 at 100KB resolution using two replicates for each experimental condition (Suhas S. P. Rao et al. 2017). Data were normalized using multiHiCcompare's cyclic loess or fastlo functions and then input into multiHiCcompare's exact test. The ROC curves indicate that the normalization methods are about equivalent for the purpose of comparison.

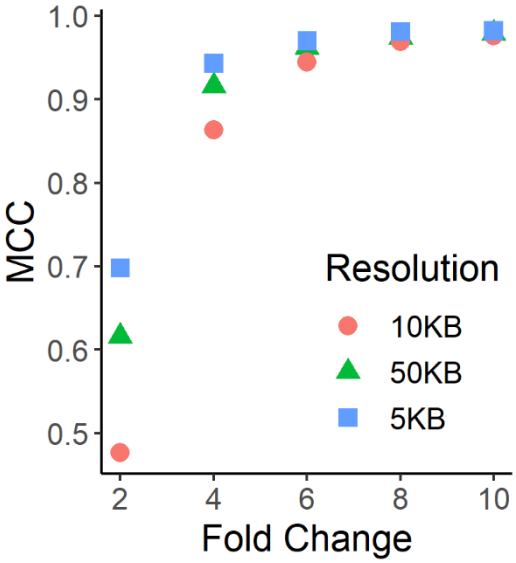

Supplemental Figure S5. Performance evaluation of multiHiCcompare over various resolutions. HCT-116 replicate data was used to perform 2x2 comparisons on the ability to detect added in true differences (see Methods). multiHiCcompare was found to be robust even at high resolution when detecting fold differences >= 4.

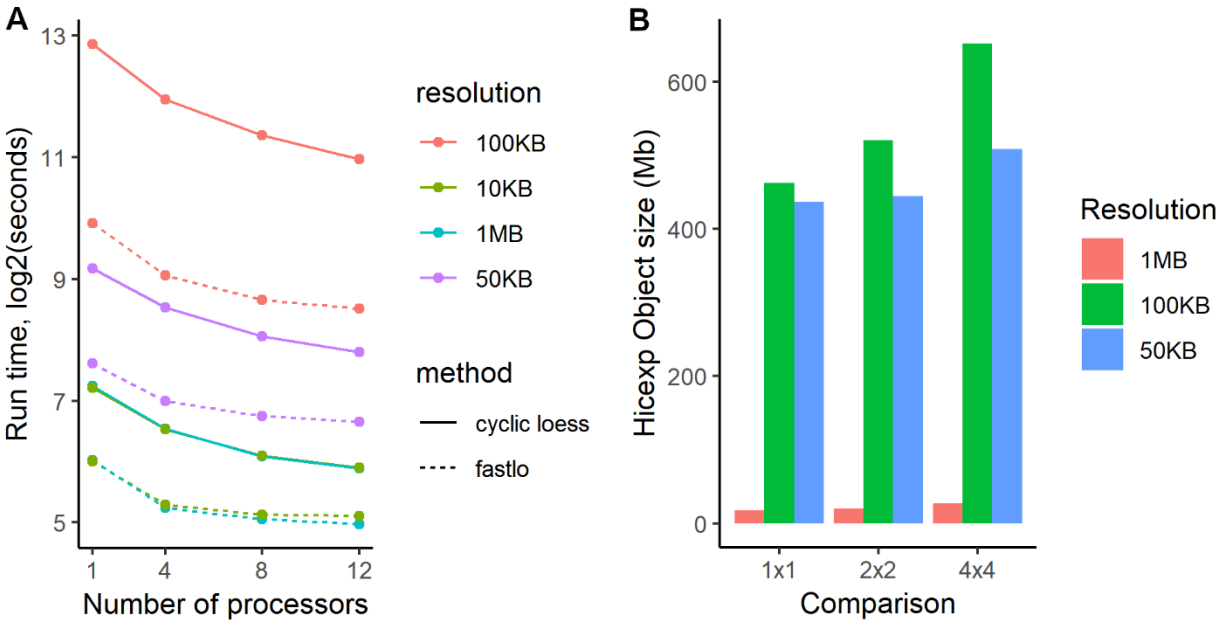

Supplemental Figure S6. A) Performance comparison between cyclic loess and fastlo normalization algorithms. The plot of computational runtime for cyclic loess and fastlo using various numbers of processors, over multiple resolutions of Hi-C data. Data used was from HCT-116 cell line (Suhas S. P. Rao et al. 2017) performing a comparison between two groups with a sample size of 2 per group on chromosomes 1-22. Run times include the normalization steps and the difference detection steps. B) Memory usage comparison for the Hicexp object used in multiHiCcompare. Comparison indicates the number of samples per group, memory usage

shown in Megabytes. Data used was from HCT-116 cell line, chromosomes 1-22 (Suhas S. P. Rao et al. 2017).

Supplemental Tables

Supplemental Table S1. Data sources used in multiHiCcompare analyses. “Library” - the Hi-C library name (hyperlink to sample on GEO); “Cell type”, “Condition” - the biological condition for the dataset.

Library	Cell type	Condition
Rao-2017-HIC001	HCT-116-RAD21-mAC	Normal; Biological Sample 1
Rao-2017-HIC002	HCT-116-RAD21-mAC	Normal; Biological Sample 1
Rao-2017-HIC003	HCT-116-RAD21-mAC	Normal; Biological Sample 1
Rao-2017-HIC004	HCT-116-RAD21-mAC	Normal; Biological Sample 2
Rao-2017-HIC005	HCT-116-RAD21-mAC	Normal; Biological Sample 2
Rao-2017-HIC006	HCT-116-RAD21-mAC	Normal; Biological Sample 2
Rao-2017-HIC007	HCT-116-RAD21-mAC	Normal; Biological Sample 2
Rao-2017-HIC008	HCT-116-RAD21-mAC	Auxin; Biological Sample 1
Rao-2017-HIC009	HCT-116-RAD21-mAC	Auxin; Biological Sample 1
Rao-2017-HIC010	HCT-116-RAD21-mAC	Auxin; Biological Sample 1
Rao-2017-HIC011	HCT-116-RAD21-mAC	Auxin; Biological Sample 2
Rao-2017-HIC012	HCT-116-RAD21-mAC	Auxin; Biological Sample 2
Rao-2017-HIC013	HCT-116-RAD21-mAC	Auxin; Biological Sample 2
Rao-2017-HIC014	HCT-116-RAD21-mAC	Auxin; Biological Sample 2
Rickman 2012	RWPE1	ERG library 1
Rickman 2012	RWPE1	ERG library 2
Rickman 2012	RWPE1	GFP library 1
Rickman 2012	RWPE1	GFP library 2
Zuin 2013	HEK293	siRNA Control 1
Zuin 2013	HEK293	siRNA Control 2
Zuin 2013	HEK293	siRNA CTCF 1
Zuin 2013	HEK293	siRNA CTCF 2

Supplemental Table S2. Comparison of multiHiCcompare and FIND over various fold changes and numbers of replicates per group using standard performance classifiers. Performance classifier methods used are "TP" - true positives, "FP" - false positives, "TN" - true negatives, "FN" - false negatives, "TPR" - True Positive Rate, aka recall, or sensitivity $TP/(TP+FN)$, "SPC" - specificity, $TN/(FP+TN)$, "F1" - F_1 score, $2TP/(2TP+FP+FN)$, "Accuracy" - $(TP+TN)/(TP+FP+TN+FN)$, "Precision" - $TP/(TP+FP)$, "FPR" - False Positive Rate, $FP/(FP+TN)$, "FNR" - False Negative Rate, $FN/(TP+FN)$, "FOR" - False omission rate, $FN/(FN+TN)$, "NPV" - Negative Predictive Value, $TN/(FN+TN)$, "MCC" - Matthews correlation coefficient, $\frac{TP\times TN-FP\times FN}{\sqrt{(TP+FP)(TP+FN)(TN+FP)(TN+FN)}}$, "F1" - $2*(\frac{TP}{TP+FP}*Precision)/(\frac{TP}{TP+FP}+Precision)$

Fold Change	Comparison	Method	Total	TPR	SPC	FDR	Accuracy	Precision	FPR	FNR	FOR	NPV	MCC	F1
2	**2x2**	**multiHiCcompare**	90000	1	1	0	0.995	1	0	0.89	0.005	0.995	0.33	0.197
		FIND	90000	0.508	0.998	0.492	0.994	0.508	0.002	0.639	0.004	0.996	0.425	0.422
	3x3	**multiHiCcompare**	90000	0.982	1	0.018	0.997	0.982	0	0.552	0.003	0.997	0.662	0.615
		FIND	90000	0.496	0.998	0.504	0.994	0.496	0.002	0.646	0.004	0.996	0.416	0.413
	4x4	**multiHiCcompare**	90000	0.957	1	0.043	0.997	0.957	0	0.509	0.003	0.997	0.684	0.649
		FIND	90000	0.742	0.999	0.258	0.996	0.742	0.001	0.455	0.003	0.997	0.634	0.629
4	**2x2**	**multiHiCcompare**	90000	0.977	1	0.023	0.997	0.977	0	0.486	0.003	0.997	0.708	0.674
		FIND	90000	0.704	0.999	0.296	0.996	0.704	0.001	0.486	0.003	0.997	0.6	0.594
	3x3	**multiHiCcompare**	90000	0.976	1	0.024	0.998	0.976	0	0.352	0.002	0.998	0.795	0.779
		FIND	90000	0.786	0.999	0.214	0.997	0.786	0.001	0.436	0.002	0.998	0.664	0.656
	4x4	**multiHiCcompare**	90000	0.948	1	0.052	0.997	0.948	0	0.492	0.003	0.997	0.693	0.661
		FIND	90000	0.646	0.999	0.354	0.996	0.646	0.001	0.53	0.003	0.997	0.549	0.544
6	**2x2**	**multiHiCcompare**	90000	0.961	1	0.039	0.999	0.961	0	0.168	0.001	0.999	0.894	0.892
		FIND	90000	0.747	0.999	0.253	0.996	0.747	0.001	0.464	0.003	0.997	0.631	0.624
	3x3	**multiHiCcompare**	90000	0.963	1	0.037	0.997	0.963	0	0.47	0.003	0.997	0.713	0.683
		FIND	90000	0.501	0.998	0.499	0.995	0.501	0.002	0.633	0.003	0.997	0.426	0.424
	4x4	**multiHiCcompare**	90000	0.96	1	0.04	0.996	0.96	0	0.658	0.004	0.996	0.572	0.504
		FIND	90000	0.744	0.999	0.256	0.996	0.744	0.001	0.463	0.003	0.997	0.63	0.624

Supplemental Table S3. Analysis of transcription factor enrichment in regions detected by multiHiCcompare, HCT-116 colon cancer cell line (Suhas S. P. Rao et al. 2017). Data source - CistromeDB. “Accession number” - GEO accession number; “Transcription Factor” - the protein for which ChIP-seq was performed, “Filename” - the filename for the ChIP-seq peaks, “Mean logFC” - the average log2 fold change for the difference between auxin and normal as determined by multiHiCcompare; “p-value” - the permutation p-value for the test of enrichment in the regions detected by multiHiCcompare.

Accession number	Transcription Factor	Filename	Mean logFC	p-value
GSM749823	AFF4	1140_sort_peaks.narrowPeak.bed	-0.7823	9.990E-04
GSM749819	AFF4	1141_sort_peaks.narrowPeak.bed	-0.4494	6.993E-03
GSM1162745	AFF4	39916_sort_peaks.narrowPeak.bed	0.1975	5.994E-03
GSM1727069	AFF4	55639_sort_peaks.narrowPeak.bed	-0.0508	4.905E-01
GSM1727070	AFF4	55640_sort_peaks.narrowPeak.bed	-0.3941	7.163E-01
GSM1727071	AFF4	55641_sort_peaks.narrowPeak.bed	0.0855	6.823E-01
GSM1727072	AFF4	55642_sort_peaks.narrowPeak.bed	0.0427	9.960E-01
GSM1010757	ATF3	46217_sort_peaks.narrowPeak.bed	-0.7915	2.997E-03
GSM1010758	CBX3	46209_sort_peaks.narrowPeak.bed	-0.8888	9.990E-04
GSM699727	CBX3	9228_sort_peaks.narrowPeak.bed	-0.7562	9.990E-04
GSM699729	CBX3	9230_sort_peaks.narrowPeak.bed	-0.8942	9.990E-04
GSM699734	CBX3	9231_sort_peaks.narrowPeak.bed	-0.7269	5.834E-01
GSM699735	CBX3	9232_sort_peaks.narrowPeak.bed	-0.9280	1.099E-02
GSM898224	CBX3	9236_sort_peaks.narrowPeak.bed	0.0234	9.640E-01
GSM898225	CBX3	9237_sort_peaks.narrowPeak.bed	-0.0164	6.773E-01
GSM1727073	CDK9	55643_sort_peaks.narrowPeak.bed	-0.3280	5.554E-01
GSM1727074	CDK9	55644_sort_peaks.narrowPeak.bed	-0.2649	8.402E-01
GSM1866698	CDK9	57093_sort_peaks.narrowPeak.bed	-0.7208	7.123E-01
GSM1010852	CEBPB	46206_sort_peaks.narrowPeak.bed	-0.8745	9.990E-04
GSM1224649	CTCF	42148_sort_peaks.narrowPeak.bed	-0.8593	4.116E-01
GSM1224650	CTCF	42149_sort_peaks.narrowPeak.bed	-0.8703	2.018E-01
GSM1224651	CTCF	42150_sort_peaks.narrowPeak.bed	-0.8802	6.503E-01
GSM1224652	CTCF	42151_sort_peaks.narrowPeak.bed	-0.8435	7.922E-01

GSM1224653	CTCF	42152_sort_peaks.narrowPeak.bed	-0.8649	5.624E-01
GSM1224654	CTCF	42153_sort_peaks.narrowPeak.bed	-0.8223	8.701E-01
GSM1224655	CTCF	42154_sort_peaks.narrowPeak.bed	-0.8085	8.771E-01
GSM1022652	CTCF	45716_sort_peaks.narrowPeak.bed	-0.8704	1.768E-01
GSM1022651	CTCF	45717_sort_peaks.narrowPeak.bed	-0.8600	4.246E-01
GSM1010903	CTCF	46218_sort_peaks.narrowPeak.bed	-0.8534	9.491E-02
GSM1010846	EGR1	46214_sort_peaks.narrowPeak.bed	-0.7530	2.098E-02
GSM1010765	ELF1	46202_sort_peaks.narrowPeak.bed	-0.7571	1.099E-02
GSM1162746	ELL	39915_sort_peaks.narrowPeak.bed	-0.1672	8.062E-01
GSM749822	ELL2	1143_sort_peaks.narrowPeak.bed	-0.7715	2.338E-01
GSM749818	ELL2	1144_sort_peaks.narrowPeak.bed	-0.8095	1.229E-01
GSM1727075	ELL2	55645_sort_peaks.narrowPeak.bed	-0.4045	5.285E-01
GSM1727076	ELL2	55646_sort_peaks.narrowPeak.bed	-0.6241	8.991E-01
GSM1727077	ELL2	55647_sort_peaks.narrowPeak.bed	-0.2366	3.167E-01
GSM1727078	ELL2	55648_sort_peaks.narrowPeak.bed	-0.6525	9.261E-01
GSM1240110	EP300	42907_sort_peaks.narrowPeak.bed	-0.8923	9.990E-04
GSM1010756	FOSL1	46212_sort_peaks.narrowPeak.bed	-0.8909	9.990E-04
GSM1535696	HNF4A	54660_sort_peaks.narrowPeak.bed	-0.7359	6.004E-01
GSM1535701	HNF4A	54665_sort_peaks.narrowPeak.bed	-0.7547	7.383E-01
GSM1535702	HNF4A	54666_sort_peaks.narrowPeak.bed	-0.7600	3.027E-01
GSM1535709	HNF4A	54673_sort_peaks.narrowPeak.bed	-0.9325	3.097E-02
GSM1535710	HNF4A	54674_sort_peaks.narrowPeak.bed	-0.9759	4.296E-02
GSM1382049	HSF1	51107_sort_peaks.narrowPeak.bed	-0.7577	9.281E-01
GSM1382050	HSF1	51108_sort_peaks.narrowPeak.bed	-0.7158	8.462E-01
GSM1382052	HSF1	51110_sort_peaks.narrowPeak.bed	-0.6184	9.740E-01
GSM1382054	HSF1	51112_sort_peaks.narrowPeak.bed	-0.2609	9.860E-01
GSM1382055	HSF1	51113_sort_peaks.narrowPeak.bed	0.2973	9.670E-01
GSM1382057	HSF1	51115_sort_peaks.narrowPeak.bed	-0.4209	9.381E-01
GSM1010847	JUND	46213_sort_peaks.narrowPeak.bed	-0.8686	9.990E-04

GSM1240109	KMT2B	42906_sort_peaks.narrowPeak.bed	-0.8358	9.990E-04
GSM1866696	LARP7	57091_sort_peaks.narrowPeak.bed	-0.6278	9.101E-01
GSM1727091	LEO1	55661_sort_peaks.narrowPeak.bed	-0.1623	2.368E-01
GSM1010904	MAX	46216_sort_peaks.narrowPeak.bed	-0.8191	9.990E-04
GSM1154509	MECP2	34399_sort_peaks.narrowPeak.bed	-0.8212	1.598E-02
GSM1154510	MECP2	34400_sort_peaks.narrowPeak.bed	-0.8802	4.236E-01
GSM1727090	NR0B2	55660_sort_peaks.narrowPeak.bed	0.1713	1.219E-01
GSM1727094	PAF1	55664_sort_peaks.narrowPeak.bed	-0.6079	4.895E-01
GSM1727095	PAF1	55665_sort_peaks.narrowPeak.bed	-0.5583	6.164E-01
GSM1727096	PAF1	55666_sort_peaks.narrowPeak.bed	-0.4464	4.925E-01
GSM1727097	PAF1	55667_sort_peaks.narrowPeak.bed	-0.6220	5.594E-02
GSM1727098	PAF1	55668_sort_peaks.narrowPeak.bed	-0.5813	6.284E-01
GSM1727099	PAF1	55669_sort_peaks.narrowPeak.bed	-0.5571	6.703E-01
GSM1727106	PAF1	55676_sort_peaks.narrowPeak.bed	-0.0116	6.484E-01
GSM749821	POLR2A	1151_sort_peaks.narrowPeak.bed	-0.6489	1.848E-01
GSM749817	POLR2A	1152_sort_peaks.narrowPeak.bed	-0.6357	4.685E-01
GSM1154513	POLR2A	34398_sort_peaks.narrowPeak.bed	-0.7408	2.587E-01
GSM1162752	POLR2A	39917_sort_peaks.narrowPeak.bed	-0.6931	3.696E-02
GSM1162755	POLR2A	39921_sort_peaks.narrowPeak.bed	-0.6969	2.198E-02
GSM935426	POLR2A	45715_sort_peaks.narrowPeak.bed	-0.5847	6.304E-01
GSM803474	POLR2A	46201_sort_peaks.narrowPeak.bed	-0.7520	4.995E-03
GSM1465032	POLR2A	49533_sort_peaks.narrowPeak.bed	-0.4726	8.591E-01
GSM1465033	POLR2A	49534_sort_peaks.narrowPeak.bed	-0.5088	9.780E-01
GSM1465034	POLR2A	49535_sort_peaks.narrowPeak.bed	-0.5791	5.285E-01
GSM1727092	POLR2A	55662_sort_peaks.narrowPeak.bed	-0.4742	3.606E-01
GSM1727093	POLR2A	55663_sort_peaks.narrowPeak.bed	-0.4969	8.761E-01
GSM1727100	POLR2A	55670_sort_peaks.narrowPeak.bed	-0.2656	6.943E-01
GSM1727101	POLR2A	55671_sort_peaks.narrowPeak.bed	-0.5959	4.705E-01
GSM1727102	POLR2A	55672_sort_peaks.narrowPeak.bed	-0.4995	7.173E-01

GSM1727103	POLR2A	55673_sort_peaks.narrowPeak.bed	-0.4935	8.282E-01
GSM1727104	POLR2A	55674_sort_peaks.narrowPeak.bed	-0.5530	3.327E-01
GSM1727105	POLR2A	55675_sort_peaks.narrowPeak.bed	-0.5883	7.273E-01
GSM1727107	POLR2A	55677_sort_peaks.narrowPeak.bed	-0.1744	9.600E-01
GSM1727108	POLR2A	55678_sort_peaks.narrowPeak.bed	0.0674	9.540E-01
GSM1727109	POLR2A	55679_sort_peaks.narrowPeak.bed	-0.0059	9.790E-01
GSM1727110	POLR2A	55680_sort_peaks.narrowPeak.bed	0.4066	6.893E-01
GSM833286	POLR2A	5661_sort_peaks.narrowPeak.bed	-0.6167	5.804E-01
GSM1866693	POLR2A	57088_sort_peaks.narrowPeak.bed	-0.4551	9.720E-01
GSM1866694	POLR2A	57089_sort_peaks.narrowPeak.bed	-0.5729	5.205E-01
GSM1010848	RAD21	46207_sort_peaks.narrowPeak.bed	-0.8674	9.990E-04
GSM1010869	REST	46203_sort_peaks.narrowPeak.bed	-0.6385	1.369E-01
GSM1010905	SIN3A	46208_sort_peaks.narrowPeak.bed	-0.7064	6.294E-02
GSM2809611	SMC1A	85289_peaks.bed	-0.8489	4.396E-02
GSM1010902	SP1	46215_sort_peaks.narrowPeak.bed	-0.8675	9.990E-04
GSM855444	SP1	5390_sort_peaks.narrowPeak.bed	-1.7630	8.991E-02
GSM855445	SP1	5391_sort_peaks.narrowPeak.bed	-1.2849	9.790E-02
GSM855447	SP1	5393_sort_peaks.narrowPeak.bed	-1.1784	4.176E-01
GSM855449	SP1	5395_sort_peaks.narrowPeak.bed	-0.5384	9.830E-01
GSM1010851	SRF	46211_sort_peaks.narrowPeak.bed	-0.8295	9.990E-04
GSM1535697	TCF4	54661_sort_peaks.narrowPeak.bed	-1.0047	9.990E-04
GSM1535698	TCF4	54662_sort_peaks.narrowPeak.bed	-1.0736	9.391E-02
GSM1535699	TCF4	54663_sort_peaks.narrowPeak.bed	-1.0455	1.998E-02
GSM1535700	TCF4	54664_sort_peaks.narrowPeak.bed	-1.0548	3.297E-02
GSM1535703	TCF4	54667_sort_peaks.narrowPeak.bed	-1.0732	2.997E-03
GSM1535704	TCF4	54668_sort_peaks.narrowPeak.bed	-1.3284	2.737E-01
GSM1535705	TCF4	54669_sort_peaks.narrowPeak.bed	-0.9754	1.109E-01
GSM1535706	TCF4	54670_sort_peaks.narrowPeak.bed	-1.0073	4.795E-02
GSM782123	TCF7L2	45714_sort_peaks.narrowPeak.bed	-0.8291	9.990E-04

GSM1010772	TEAD4	46210_sort_peaks.narrowPeak.bed	-0.8177	9.990E-04
GSM1152879	TET2	50981_sort_peaks.narrowPeak.bed	-0.4797	8.382E-01
GSM1412743	TP53	50344_sort_peaks.narrowPeak.bed	-1.2044	6.943E-01
GSM1412744	TP53	50345_sort_peaks.narrowPeak.bed	-1.0012	8.392E-02
GSM1417250	TP53	50346_sort_peaks.narrowPeak.bed	-1.1125	5.315E-01
GSM1468849	TP53	53285_sort_peaks.narrowPeak.bed	-1.0594	7.043E-01
GSM1468850	TP53	53286_sort_peaks.narrowPeak.bed	-0.9280	5.704E-01
GSM1866695	TRIM28	57090_sort_peaks.narrowPeak.bed	-0.6549	9.970E-01
GSM1010836	USF1	46205_sort_peaks.narrowPeak.bed	-0.7887	1.998E-03
GSM1165982	USP49	39345_sort_peaks.narrowPeak.bed	0.0264	9.111E-01
GSM1165983	USP49	39347_sort_peaks.narrowPeak.bed	-0.2937	9.890E-01
GSM803354	YY1	46204_sort_peaks.narrowPeak.bed	-0.7807	1.099E-02
GSM803458	ZBTB33	46200_sort_peaks.narrowPeak.bed	-0.5795	3.996E-03
GSM1162749	ZC3H8	39918_sort_peaks.narrowPeak.bed	-0.7304	6.993E-03

Supplemental Table S4. Analysis of multiHiCcompare performance over various resolutions and at various fold changes for added in differences. Data from HCT-116 cell lines at resolutions of 50KB, 10KB, and 5KB from chromosome 18. Performance classifier methods used are "TP" - true positives, "FP" - false positives, "TN" - true negatives, "FN" - false negatives, "TPR" - True Positive Rate, aka recall, or sensitivity $TP/(TP+FN)$, "SPC" - specificity, $TN/(FP+TN)$, "F1" - F_1 score, $2TP/(2TP+FP+FN)$, "Accuracy" - $(TP+TN)/(TP+FP+TN+FN)$, "Precision" - $TP/(TP+FP)$, "FPR" - False Positive Rate, $FP/(FP+TN)$, "FNR" - False Negative Rate, $FN/(TP+FN)$, "FOR" - False omission rate, $FN/(FN+TN)$, "NPV" - Negative Predictive Value, $TN/(FN+TN)$, "MCC" - Matthews correlation coefficient, $\frac{TP\times TN-FP\times FN}{\sqrt{(TP+FP)(TP+FN)(TN+FP)(TN+FN)}}$, "F1" - $2*(\frac{TP}{TP+FP}*Precision)/(\frac{TP}{TP+FP}+Precision)$

Measure	TP	FP	TN	FN	F1	AUC	FDR	Accuracy	Precision	FPR	FNR	FOR	NPV	MCC
50KB; FC=2	2011	57	77117	2989	0.569	0.865	0.963	0.963	0.972	0.001	0.598	0.037	0.963	0.613
50KB; FC=4	4404	103	77071	596	0.926	0.989	0.991	0.991	0.977	0.001	0.119	0.008	0.992	0.923
50KB; FC=6	4782	121	77053	218	0.966	0.997	0.996	0.996	0.975	0.002	0.044	0.003	0.997	0.964
10KB; FC=2	1267	41	65802	3733	0.402	0.81	0.947	0.947	0.969	0.001	0.747	0.054	0.946	0.481
10KB; FC=4	3942	115	65728	1058	0.87	0.982	0.983	0.983	0.972	0.002	0.212	0.016	0.984	0.867
10KB; FC=6	4653	142	65701	347	0.95	0.996	0.993	0.993	0.97	0.002	0.069	0.005	0.995	0.947
5KB; FC=2	2659	40	30362	2341	0.691	0.911	0.933	0.933	0.985	0.001	0.468	0.072	0.928	0.696
5KB; FC=4	4573	93	30309	427	0.946	0.992	0.985	0.985	0.98	0.003	0.085	0.014	0.986	0.938
5KB; FC=6	4862	111	30291	138	0.975	0.997	0.993	0.993	0.978	0.004	0.028	0.005	0.995	0.971

Supplemental Table S5. Analysis of transcription factor enrichment in regions detected by multiHiCcompare, HEK293 cell line (Zuin et al. 2013). Data source - CistromeDB. "Accession number" - GEO accession number; "Transcription Factor" - the protein for which ChIP-seq was performed, "Filename" - the filename for the ChIP-seq peaks, "Mean logFC" - the average log2 fold change for the difference between auxin and normal as determined by multiHiCcompare; "p-value" - the permutation p-value for the test of enrichment in the regions detected by multiHiCcompare.

Accession number	Transcription Factor	Filename	Mean logFC	p-value
GSM520382	PHF8	93_sort_peaks.narrowPeak.bed	2.3149	9.99E-04
GSM509047	POLR3G	1168_sort_peaks.narrowPeak.bed	-4.0542	4.64E-01
GSM700361	ELK4	1172_sort_peaks.narrowPeak.bed	1.3192	2.00E-03
GSM700360	ELK4	1173_sort_peaks.narrowPeak.bed	0.7415	9.99E-04
GSM700357	TRIM28	1174_sort_peaks.narrowPeak.bed	2.9604	9.99E-04
GSM700356	TRIM28	1175_sort_peaks.narrowPeak.bed	3.2611	9.99E-04
GSM700355	TRIM28	1176_sort_peaks.narrowPeak.bed	0.9149	9.99E-04
GSM700354	TRIM28	1177_sort_peaks.narrowPeak.bed	5.3508	3.00E-03

GSM700353	TRIM28	1178_sort_peaks.narrowPeak.bed	3.2052	9.99E-04
GSM301567	POLR2A	1191_sort_peaks.narrowPeak.bed	2.3045	9.99E-04
GSM301566	POLR2A	1192_sort_peaks.narrowPeak.bed	2.7456	9.99E-04
GSM700359	TRIM28	1194_sort_peaks.narrowPeak.bed	3.0933	9.99E-04
GSM700358	TRIM28	1195_sort_peaks.narrowPeak.bed	3.2831	9.99E-04
GSM301581	POLR2A	2642_sort_peaks.narrowPeak.bed	3.2945	9.99E-04
GSM301568	POLR2A	2643_sort_peaks.narrowPeak.bed	3.1398	9.99E-04
GSM855007	RNF2	8549_sort_peaks.narrowPeak.bed	2.0241	9.99E-04
GSM855008	RYBP	8550_sort_peaks.narrowPeak.bed	1.9526	9.99E-04
GSM855010	PCGF2	8552_sort_peaks.narrowPeak.bed	-0.4727	7.79E-02
GSM855011	BMI1	8553_sort_peaks.narrowPeak.bed	2.1225	3.00E-03
GSM855013	PCGF6	8555_sort_peaks.narrowPeak.bed	5.5337	3.10E-02
GSM855014	CBX2	8556_sort_peaks.narrowPeak.bed	8.9304	1.50E-01
GSM855017	RNF2	8559_sort_peaks.narrowPeak.bed	-2.7727	1.11E-01
GSM855018	RYBP	8560_sort_peaks.narrowPeak.bed	-0.875	6.29E-02
GSM855019	BMI1	8561_sort_peaks.narrowPeak.bed	4.3306	1.85E-01
GSM855020	CBX2	8562_sort_peaks.narrowPeak.bed	3.4874	5.67E-01
GSM865742	GPS2	8563_sort_peaks.narrowPeak.bed	1.9827	8.29E-01
GSM865743	TBL1X	8564_sort_peaks.narrowPeak.bed	2.2675	9.99E-04
GSM865744	NCOR1	8565_sort_peaks.narrowPeak.bed	3.6005	9.99E-04
GSM865745	NCOR1	8566_sort_peaks.narrowPeak.bed	2.8181	9.99E-04
GSM897577	TET3	33988_sort_peaks.narrowPeak.bed	2.2432	9.99E-04
GSM897576	TET2	33992_sort_peaks.narrowPeak.bed	3.0843	9.99E-04
GSM1054011	MYC	34317_sort_peaks.narrowPeak.bed	2.7853	7.49E-02
GSM1054009	MYC	34318_sort_peaks.narrowPeak.bed	2.4976	9.99E-04
GSM1054010	MYC	34319_sort_peaks.narrowPeak.bed	3.3474	1.20E-01
GSM1050111	GCG	34532_sort_peaks.narrowPeak.bed	2.904	6.79E-02
GSM1050110	EHMT2	34535_sort_peaks.narrowPeak.bed	3.6662	5.09E-02
GSM971947	BRD3	35874_sort_peaks.narrowPeak.bed	1.4877	9.99E-04
GSM971949	CBX5	35875_sort_peaks.narrowPeak.bed	6.6305	6.39E-02
GSM971948	BRD4	35876_sort_peaks.narrowPeak.bed	-0.9776	1.10E-02
GSM971946	BRD2	35878_sort_peaks.narrowPeak.bed	2.7475	9.99E-04
GSM971950	CBX1	35879_sort_peaks.narrowPeak.bed	4.3306	2.37E-01
GSM1140398	FANCD2	36113_sort_peaks.narrowPeak.bed	4.1734	8.19E-02
GSM1140397	FANCD2	36114_sort_peaks.narrowPeak.bed	2.6222	9.99E-04
GSM891243	DCP1A	36226_sort_peaks.narrowPeak.bed	2.7263	9.99E-04
GSM891244	POLR2A	36227_sort_peaks.narrowPeak.bed	3.7736	9.99E-04
GSM891241	XRN2	36228_sort_peaks.narrowPeak.bed	2.3776	9.99E-04
GSM891239	TTF2	36230_sort_peaks.narrowPeak.bed	2.6618	9.99E-04
GSM891240	XRN2	36234_sort_peaks.narrowPeak.bed	2.372	9.99E-04
GSM891242	POLR2A	36235_sort_peaks.narrowPeak.bed	2.2812	9.99E-04
GSM1151769	YBX1	36659_sort_peaks.narrowPeak.bed	2.0411	8.99E-02
GSM959048	ZNF143	36766_sort_peaks.narrowPeak.bed	3.3148	9.99E-04
GSM841736	AFF4	38227_sort_peaks.narrowPeak.bed	0.9309	3.50E-02
GSM1018960	TET3	39719_sort_peaks.narrowPeak.bed	2.9154	9.99E-04

GSM1037511	HCFC1	39886_sort_peaks.narrowPeak.bed	2.5906	9.99E-04
GSM844016	POLR2A	39930_sort_peaks.narrowPeak.bed	2.7942	9.99E-04
GSM1081542	SMC3	41382_sort_peaks.narrowPeak.bed	2.7747	9.99E-04
GSM1176699	NR3C1	41735_sort_peaks.narrowPeak.bed	2.8303	9.99E-04
GSM1176700	NR3C1	41736_sort_peaks.narrowPeak.bed	10.8515	1.16E-01
GSM1176701	NR3C1	41737_sort_peaks.narrowPeak.bed	2.7793	3.50E-02
GSM1176702	NR3C1	41738_sort_peaks.narrowPeak.bed	2.366	9.99E-01
GSM1215133	EZH2	41974_sort_peaks.narrowPeak.bed	1.5614	4.67E-01
GSM1220022	BRD4	42100_sort_peaks.narrowPeak.bed	5.455	4.00E-02
GSM1220024	BRD4	42102_sort_peaks.narrowPeak.bed	6.8626	5.79E-02
GSM1239069	EP300	42633_sort_peaks.narrowPeak.bed	2.5434	9.99E-04
GSM1239070	EP300	42634_sort_peaks.narrowPeak.bed	2.7823	9.99E-04
GSM1239073	CREBBP	42637_sort_peaks.narrowPeak.bed	2.6844	9.99E-04
GSM1239074	CREBBP	42638_sort_peaks.narrowPeak.bed	2.8931	9.99E-04
GSM1249879	JMJD6	43063_sort_peaks.narrowPeak.bed	2.389	9.99E-04
GSM1249880	JMJD6	43064_sort_peaks.narrowPeak.bed	2.5348	9.99E-04
GSM1249881	BRD4	43065_sort_peaks.narrowPeak.bed	2.0311	9.99E-04
GSM1249882	BRD4	43066_sort_peaks.narrowPeak.bed	2.6503	9.99E-04
GSM1249890	EP300	43074_sort_peaks.narrowPeak.bed	3.4132	9.99E-04
GSM1249891	POLR2A	43075_sort_peaks.narrowPeak.bed	2.7784	9.99E-04
GSM1249892	POLR2A	43076_sort_peaks.narrowPeak.bed	0.655	6.99E-03
GSM1249893	POLR2A	43077_sort_peaks.narrowPeak.bed	2.4636	9.99E-04
GSM1249894	POLR2A	43078_sort_peaks.narrowPeak.bed	2.5297	9.99E-04
GSM1249895	POLR2A	43079_sort_peaks.narrowPeak.bed	2.6567	9.99E-04
GSM1249896	POLR2A	43080_sort_peaks.narrowPeak.bed	2.5128	9.99E-04
GSM1249897	CDK9	43081_sort_peaks.narrowPeak.bed	2.4019	9.99E-04
GSM1249898	CDK9	43082_sort_peaks.narrowPeak.bed	1.6415	9.99E-04
GSM1249899	CDK9	43083_sort_peaks.narrowPeak.bed	2.8068	9.99E-04
GSM1294929	EZH2	43542_sort_peaks.narrowPeak.bed	4.0547	1.75E-01
GSM1294931	EZH2	43544_sort_peaks.narrowPeak.bed	5.0136	3.90E-01
GSM1294933	C10orf12	43546_sort_peaks.narrowPeak.bed	4.3306	7.19E-02
GSM1294935	C10orf12	43548_sort_peaks.narrowPeak.bed	4.3306	9.49E-02
GSM1294937	C17orf96	43550_sort_peaks.narrowPeak.bed	4.7975	2.00E-03
GSM1294939	C17orf96	43552_sort_peaks.narrowPeak.bed	3.8213	9.99E-03
GSM1294942	CBX4	43555_sort_peaks.narrowPeak.bed	1.1606	9.99E-04
GSM1301133	DPPA2	43668_sort_peaks.narrowPeak.bed	3.1886	9.99E-04
GSM1301134	TET3	43669_sort_peaks.narrowPeak.bed	2.9494	9.99E-04
GSM749668	CTCF	45720_sort_peaks.narrowPeak.bed	2.8618	9.99E-04
GSM749687	CTCF	45721_sort_peaks.narrowPeak.bed	2.6487	9.99E-04
GSM935534	POLR2A	45722_sort_peaks.narrowPeak.bed	2.5549	9.99E-04
GSM782124	TCF7L2	45723_sort_peaks.narrowPeak.bed	2.0938	9.68E-01
GSM935590	ELK4	45724_sort_peaks.narrowPeak.bed	1.2037	9.99E-04
GSM935592	TRIM28	45725_sort_peaks.narrowPeak.bed	3.0235	9.99E-04
GSM935577	ZNF263	45726_sort_peaks.narrowPeak.bed	2.9817	9.99E-04
GSM1192069	POLR2A	47398_sort_peaks.narrowPeak.bed	1.1574	9.99E-04

GSM1192071	POLR2A	47400_sort_peaks.narrowPeak.bed	2.474	9.99E-04
GSM1192073	POLR2A	47402_sort_peaks.narrowPeak.bed	2.5683	9.99E-04
GSM1192076	POLR2A	47405_sort_peaks.narrowPeak.bed	2.8973	9.99E-04
GSM1192077	POLR2A	47406_sort_peaks.narrowPeak.bed	2.7728	9.99E-04
GSM1308228	AR	48084_sort_peaks.narrowPeak.bed	4.3306	1.46E-01
GSM1308229	AR	48085_sort_peaks.narrowPeak.bed	2.9077	3.96E-01
GSM1308230	AR	48086_sort_peaks.narrowPeak.bed	2.8914	5.86E-01
GSM1308231	AR	48087_sort_peaks.narrowPeak.bed	7.6177	2.00E-01
GSM1308232	AR	48088_sort_peaks.narrowPeak.bed	2.9353	9.56E-01
GSM1308233	AR	48089_sort_peaks.narrowPeak.bed	2.7766	8.28E-01
GSM1414504	EMX1	49178_sort_peaks.narrowPeak.bed	2.7719	5.00E-03
GSM1414505	EMX1	49179_sort_peaks.narrowPeak.bed	4.2928	2.90E-02
GSM1416527	F2RL1	49198_sort_peaks.narrowPeak.bed	8.9304	1.47E-01
GSM1369392	DDX21	50210_sort_peaks.narrowPeak.bed	2.7353	9.99E-04
GSM1531550	POLR2A	51772_sort_peaks.narrowPeak.bed	2.5911	9.99E-04
GSM1493018	MYC	52424_sort_peaks.narrowPeak.bed	3.7759	9.99E-04
GSM1493019	MYC	52425_sort_peaks.narrowPeak.bed	5.1215	3.30E-02
GSM1493021	MYC	52427_sort_peaks.narrowPeak.bed	2.2677	9.99E-04
GSM1493022	MYC	52428_sort_peaks.narrowPeak.bed	2.4513	2.00E-03
GSM1493023	MYC	52429_sort_peaks.narrowPeak.bed	2.6239	9.99E-04
GSM1493024	MYC	52430_sort_peaks.narrowPeak.bed	8.1957	8.39E-02
GSM1493026	WDR5	52432_sort_peaks.narrowPeak.bed	2.7987	9.99E-04
GSM1493028	WDR5	52434_sort_peaks.narrowPeak.bed	5.2654	2.00E-03
GSM1493030	WDR5	52436_sort_peaks.narrowPeak.bed	2.7443	9.99E-04
GSM1530051	EHMT2	52585_sort_peaks.narrowPeak.bed	4.3306	6.39E-02
GSM1530052	ZNF644	52586_sort_peaks.narrowPeak.bed	4.3306	9.49E-02
GSM1464011	FOXM1	53251_sort_peaks.narrowPeak.bed	2.3267	9.99E-04
GSM1464012	FOXM1	53252_sort_peaks.narrowPeak.bed	2.3477	3.00E-03
GSM1464013	FOXM1	53253_sort_peaks.narrowPeak.bed	3.3634	9.99E-04
GSM1464014	FOXM1	53254_sort_peaks.narrowPeak.bed	2.9099	9.99E-04
GSM1464016	FOXM1	53256_sort_peaks.narrowPeak.bed	2.5358	9.99E-04
GSM1464017	FOXM1	53257_sort_peaks.narrowPeak.bed	1.9616	9.99E-04
GSM1464019	FOXM1	53259_sort_peaks.narrowPeak.bed	3.1531	9.99E-04
GSM1464020	FOXM1	53260_sort_peaks.narrowPeak.bed	2.9568	9.99E-04
GSM1464021	FOXM1	53261_sort_peaks.narrowPeak.bed	1.7187	9.99E-04
GSM1464022	FOXM1	53262_sort_peaks.narrowPeak.bed	2.1324	9.99E-04
GSM1464023	FOXM1	53263_sort_peaks.narrowPeak.bed	3.5308	9.99E-04
GSM1464024	FOXM1	53264_sort_peaks.narrowPeak.bed	2.7893	9.99E-04
GSM1820477	POLR2A	55798_sort_peaks.narrowPeak.bed	2.604	9.99E-04
GSM1820478	POLR2A	55799_sort_peaks.narrowPeak.bed	2.7346	9.99E-04
GSM1820479	POLR2A	55800_sort_peaks.narrowPeak.bed	2.5206	9.99E-04
GSM1820483	POLR2A	55804_sort_peaks.narrowPeak.bed	2.6223	9.99E-04
GSM1820484	POLR2A	55805_sort_peaks.narrowPeak.bed	2.548	9.99E-04
GSM1820485	POLR2A	55806_sort_peaks.narrowPeak.bed	2.4712	9.99E-04
GSM1533742	BRD1	56279_sort_peaks.narrowPeak.bed	0.7263	5.00E-03

GSM1533743	BRD1	56280_sort_peaks.narrowPeak.bed	-0.0688	2.20E-02
GSM1533744	BRD1	56281_sort_peaks.narrowPeak.bed	8.1963	1.80E-02
GSM1533745	BRD1	56282_sort_peaks.narrowPeak.bed	4.0429	3.50E-02
GSM1644649	EHMT2	56446_sort_peaks.narrowPeak.bed	2.4287	1.00E+00
GSM1644650	EHMT2	56447_sort_peaks.narrowPeak.bed	2.9767	1.00E+00
GSM1644651	EHMT2	56448_sort_peaks.narrowPeak.bed	2.898	1.00E+00
GSM1644652	EHMT2	56449_sort_peaks.narrowPeak.bed	3.5749	1.00E+00
GSM1644657	EHMT2	56454_sort_peaks.narrowPeak.bed	2.9445	1.00E+00
GSM1644658	EHMT2	56455_sort_peaks.narrowPeak.bed	1.7354	9.99E-01
GSM1644659	EHMT2	56456_sort_peaks.narrowPeak.bed	4.2466	7.01E-01
GSM1644660	EHMT2	56457_sort_peaks.narrowPeak.bed	2.4116	1.00E+00
GSM1644665	EHMT2	56462_sort_peaks.narrowPeak.bed	3.8064	1.00E+00
GSM1644666	EHMT2	56463_sort_peaks.narrowPeak.bed	2.5533	1.00E+00
GSM1644669	EHMT2	56466_sort_peaks.narrowPeak.bed	3.8258	9.98E-01
GSM1644670	EHMT2	56467_sort_peaks.narrowPeak.bed	3.0498	7.29E-02
GSM1910998	CTCF	57284_sort_peaks.narrowPeak.bed	2.6013	9.99E-04
GSM1290241	BAHD1	57659_sort_peaks.narrowPeak.bed	2.665	1.00E+00
GSM1290243	BAHD1	57661_sort_peaks.narrowPeak.bed	3.2009	9.99E-04
GSM1290244	BAHD1	57662_sort_peaks.narrowPeak.bed	3.6607	9.99E-04
GSM1872288	POLR2A	58834_sort_peaks.narrowPeak.bed	2.2956	9.99E-04
GSM1872289	POLR2A	58835_sort_peaks.narrowPeak.bed	2.0191	9.99E-04
GSM1872290	POLR2A	58836_sort_peaks.narrowPeak.bed	2.9058	9.99E-04
GSM1872291	POLR2A	58837_sort_peaks.narrowPeak.bed	3.0267	9.99E-04
GSM1872292	POLR2A	58838_sort_peaks.narrowPeak.bed	2.2135	9.99E-04
GSM1872293	POLR2A	58839_sort_peaks.narrowPeak.bed	2.3824	9.99E-04
GSM1872294	XRN2	58840_sort_peaks.narrowPeak.bed	2.7224	9.99E-04
GSM1872295	XRN2	58841_sort_peaks.narrowPeak.bed	2.6983	9.99E-04
GSM1872296	XRN2	58842_sort_peaks.narrowPeak.bed	2.7581	9.99E-04
GSM1872297	XRN2	58843_sort_peaks.narrowPeak.bed	2.3025	9.99E-04
GSM1872298	XRN2	58844_sort_peaks.narrowPeak.bed	2.6234	9.99E-04
GSM1872299	XRN2	58845_sort_peaks.narrowPeak.bed	3.056	9.99E-04
GSM1872300	XRN2	58846_sort_peaks.narrowPeak.bed	3.3542	2.00E-03
GSM1892295	SMN1	58948_sort_peaks.narrowPeak.bed	1.4541	5.99E-02
GSM1892296	SMN1	58949_sort_peaks.narrowPeak.bed	2.2222	7.70E-01
GSM1895987	TAF15	58996_sort_peaks.narrowPeak.bed	4.3306	6.19E-02

Supplemental Table S6. Transcription factors significantly (p-value <0.05) enriched in the differentially interacting regions in HEK293 CTCF knockdown cells. See legend for Table 3.

Transcription Factor	Number of experiments	Mean logFC	Stouffer-Liptak p-value
POLR2A	32	2.5403	6.87E-68
FOXM1	12	2.6438	1.38E-26
XRN2	9	2.6961	1.77E-20
TRIM28	8	3.1365	3.34E-18
MYC	9	3.674	1.07E-12
CDK9	3	2.2834	4.33E-08
CTCF	3	2.7039	4.33E-08
EP300	3	2.913	4.33E-08
TET3	3	2.7027	4.33E-08
BRD4	5	3.2043	6.64E-08
ELK4	3	1.0881	8.45E-08
WDR5	3	3.6028	8.45E-08
BAHD1	3	3.1755	6.19E-06
CREBBP	2	2.7888	6.19E-06
JMJD6	2	2.4619	6.19E-06
NCOR1	2	3.2093	6.19E-06
BRD1	4	3.2242	1.07E-05
C17orf96	2	4.3094	1.16E-04
RYBP	2	0.5388	5.42E-04
FANCD2	2	3.3978	7.63E-04
EMX1	2	3.5324	7.82E-04
BRD2	1	2.7475	9.99E-04
BRD3	1	1.4877	9.99E-04
CBX4	1	1.1606	9.99E-04
DCP1A	1	2.7263	9.99E-04
DDX21	1	2.7353	9.99E-04
DPPA2	1	3.1886	9.99E-04
HCFC1	1	2.5906	9.99E-04
PHF8	1	2.3149	9.99E-04
SMC3	1	2.7747	9.99E-04
TBL1X	1	2.2675	9.99E-04
TET2	1	3.0843	9.99E-04
TTF2	1	2.6618	9.99E-04
ZNF143	1	3.3148	9.99E-04
ZNF263	1	2.9817	9.99E-04
RNF2	2	-0.374	1.15E-03
BMI1	2	3.2265	4.97E-03
C10orf12	2	4.3306	2.50E-02
PCGF6	1	5.5337	3.10E-02
AFF4	1	0.9309	3.50E-02

References

Anders, Simon, and Wolfgang Huber. 2010. “Differential Expression Analysis for Sequence Count Data.” *Genome Biol* 11 (10): R106. doi:10.1186/gb-2010-11-10-r106.

Auer, Paul L, and R W Doerge. 2010. “Statistical Design and Analysis of Rna Sequencing Data.” *Genetics* 185 (2): 405–16. doi:10.1534/genetics.110.114983.

Baggerly, Keith A, Li Deng, Jeffrey S Morris, and C Marcelo Aldaz. 2004. “Overdispersed Logistic Regression for Sage: Modelling Multiple Groups and Covariates.” *BMC Bioinformatics* 5 (October): 144. doi:10.1186/1471-2105-5-144.

Hansen, Kasper D, Zhijin Wu, Rafael A Irizarry, and Jeffrey T Leek. 2011. “Sequencing Technology Does Not Eliminate Biological Variability.” *Nat Biotechnol* 29 (7): 572–3. doi:10.1038/nbt.1910.

Kal, A J, A J van Zonneveld, V Benes, M van den Berg, M G Koerkamp, K Albermann, N Strack, et al. 1999. “Dynamics of Gene Expression Revealed by Comparison of Serial Analysis of Gene Expression Transcript Profiles from Yeast Grown on Two Different Carbon Sources.” *Mol Biol Cell* 10 (6): 1859–72.

Lu, Jun, John K Tomfohr, and Thomas B Kepler. 2005. “Identifying Differential Expression in Multiple Sage Libraries: An Overdispersed Log-Linear Model Approach.” *BMC Bioinformatics* 6 (June): 165. doi:10.1186/1471-2105-6-165.

McCarthy, Davis J, Yunshun Chen, and Gordon K Smyth. 2012. “Differential Expression Analysis of Multifactor Rna-Seq Experiments with Respect to Biological Variation.” *Nucleic Acids Res* 40 (10): 4288–97. doi:10.1093/nar/gks042.

Rao, Suhas S P, Miriam H Huntley, Neva C Durand, Elena K Stamenova, Ivan D Bochkov, James T Robinson, Adrian L Sanborn, et al. 2014. “A 3d Map of the Human Genome at Kilobase Resolution Reveals Principles of Chromatin Looping.” *Cell* 159 (7): 1665–80. doi:10.1016/j.cell.2014.11.021.

Rao, Suhas S. P., Su-Chen Huang, Brian Glenn St Hilaire, Jesse M. Engreitz, Elizabeth M. Perez, Kyong-Rim Kieffer-Kwon, Adrian L. Sanborn, et al. 2017. “Cohesin Loss Eliminates All Loop Domains.” *Cell* 171 (2). Elsevier: 305–320.e24. doi:10.1016/j.cell.2017.09.026.

Robinson, Mark D, and Gordon K Smyth. 2007. “Moderated Statistical Tests for Assessing Differences in Tag Abundance.” *Bioinformatics* 23 (21): 2881–7. doi:10.1093/bioinformatics/btm453.

Robinson, Mark D, and Smyth, Gordon K. 2008. “Small-Sample Estimation of Negative Binomial Dispersion, with Applications to Sage Data.” *Biostatistics* 9 (2): 321–32. doi:10.1093/biostatistics/kxm030.

Robinson, Mark D, Davis J McCarthy, and Gordon K Smyth. 2010. “EdgeR: A Bioconductor Package for Differential Expression Analysis of Digital Gene Expression Data.” *Bioinformatics* 26 (1): 139–40. doi:10.1093/bioinformatics/btp616.

Tjur, Tue. 1998. “Nonlinear Regression, Quasi Likelihood, and Overdispersion in Generalized Linear Models.” *The American Statistician* 52 (3). [American Statistical Association, Taylor & Francis, Ltd.]: 222–27. http://www.jstor.org/stable/2685928.

Zuin, J., Dixon, J. R., van der Reijden, M. I., Ye, Z., Kolovos, P., Brouwer, R. W., van de Corput, M. P., van de Werken, H. J., Knoch, T. A., van IJcken, W. F., Grosveld, F. G., Ren, B., … Wendt, K. S. (2013). Cohesin and CTCF differentially affect chromatin architecture and gene expression in human cells. *Proceedings of the National Academy of Sciences of the United States of America*